

Accepted Manuscript

Design and Synthesis of Novel Selective Anaplastic Lymphoma Kinase Inhibitors

Pierre-Yves Michellys, Bei Chen, Tao Jiang, Yunho Jin, Wenshuo Lu, Thomas H. Marsilje, Wei Pei, Tetsuo Uno, Xuefeng Zhu, Baogen Wu, Truc Ngoc Nguyen, Badry Bursulaya, Christian Lee, Nanxin Li, Sungjoon Kim, Tove Tuntland, Bo Liu, Frank Sun, Auzon Steffy, Tami Hood

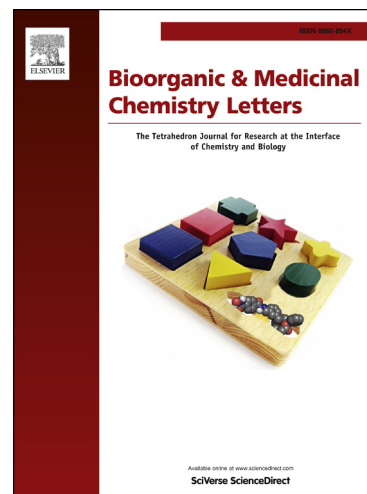
PII: S0960-894X(15)30257-2
DOI: <http://dx.doi.org/10.1016/j.bmcl.2015.11.049>
Reference: BMCL 23305

To appear in: *Bioorganic & Medicinal Chemistry Letters*

Received Date: 3 August 2015
Revised Date: 12 November 2015
Accepted Date: 16 November 2015

Please cite this article as: Michellys, P-Y., Chen, B., Jiang, T., Jin, Y., Lu, W., Marsilje, T.H., Pei, W., Uno, T., Zhu, X., Wu, B., Nguyen, T.N., Bursulaya, B., Lee, C., Li, N., Kim, S., Tuntland, T., Liu, B., Sun, F., Steffy, A., Hood, T., Design and Synthesis of Novel Selective Anaplastic Lymphoma Kinase Inhibitors, *Bioorganic & Medicinal Chemistry Letters* (2015), doi: <http://dx.doi.org/10.1016/j.bmcl.2015.11.049>

This is a PDF file of an unedited manuscript that has been accepted for publication. As a service to our customers we are providing this early version of the manuscript. The manuscript will undergo copyediting, typesetting, and review of the resulting proof before it is published in its final form. Please note that during the production process errors may be discovered which could affect the content, and all legal disclaimers that apply to the journal pertain.



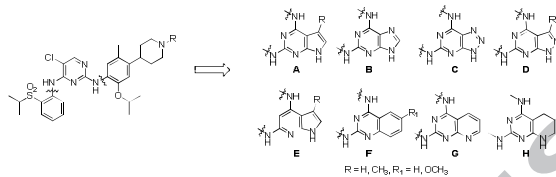
Graphical Abstract

To create your abstract, type over the instructions in the template box below.
Fonts or abstract dimensions should not be changed or altered.

Design and Synthesis of Novel Selective Anaplastic Lymphoma Kinase Inhibitors

Leave this area blank for abstract info.

Pierre-Yves Michellys, Bei Chen Tao Jiang, Yunho Jin, Wenshuo Lu, Thomas H. Marsilje, Wei Pei, Tetsuo Uno, Xuefeng Zhu, Baogen Wu, Truc Ngoc Nguyen, Badry Bursulaya, Christian Lee, Nanxin L, Sungjoon Kim, Tove Tuntland, Bo Liu, Frank Sun, Auzon Steffy and Tami Hood





Design and Synthesis of Novel Selective Anaplastic Lymphoma Kinase Inhibitors

Pierre-Yves Michellys^{a,*}, Bei Chen^a, Tao Jiang^a, Yunho Jin^a, Wenshuo Lu^a, Thomas H. Marsilje^a, Wei Pei^a, Tetsuo Uno^a, Xuefeng Zhu^a, Baogen Wu^a, Truc Ngoc Nguyen^a, Badry Bursulaya^a, Christian Lee^a, Nanxin Li^a, Sungjoon Kim^a, Tove Tuntland^a, Bo Liu^a, Frank Sun^b, Auzon Steffy^a and Tami Hood^c

^a Genomics Institute of the Novartis Research Foundation, 10675 John Jay Hopkins Drive, San Diego, CA 920121

* To whom correspondence should be addressed

^b Sanofi Oncology, 640 Memorial Drive, Cambridge, MA 02139

^c Novartis Institutes for BioMedical Research, Inc., 250 Massachusetts Avenue, Cambridge, MA 02139

ARTICLE INFO

Article history:

Received

Revised

Accepted

Available online

Keywords:

ALK

Scaffold morphing

Hinge

Karpas299

ABSTRACT

Anaplastic lymphoma kinase (ALK) is a receptor tyrosine kinase belonging to the insulin receptor superfamily. Expression of ALK in normal human tissues is only found in a subset of neural cells, however it is involved in the genesis of several cancers through genetic aberrations involving translocation of the kinase domain with multiple fusion partners (e.g. NPM-ALK in anaplastic large cell lymphoma ALCL or EML4-ALK in non-small cell lung cancer) or activating mutations in the full-length receptor resulting in ligand-independent constitutive activation (e.g. neuroblastoma). Here we are reporting the discovery of novel and selective anaplastic lymphoma kinase inhibitors from specific modifications of the 2,4-diaminopyridine core present in TAE684 and LDK378. Synthesis, structure activity relationships (SAR), absorption, distribution, metabolism, and excretion (ADME) profile, and *in vivo* efficacy in a mouse xenograft model of anaplastic large cell lymphoma are described.

2009 Elsevier Ltd. All rights reserved.

Anaplastic lymphoma kinase (ALK) is a receptor tyrosine kinase of the insulin receptor superfamily and expression of ALK in normal human tissues is only found in a subset of neural cells.¹ It is involved however in the genesis of several cancers through genetic aberrations involving translocation of the kinase domain with multiple fusion partners or activating mutations that result in ligand-independent constitutive activation.²⁻⁴ To date, no essential role has been found for ALK in mammals. Mice deficient in ALK have normal development and display an anti-depressive profile with enhanced performance in hippocampus-dependent tasks potentially due to increased hippocampal progenitor cells.⁵

Deregulation of ALK was first identified in anaplastic large cell lymphoma (ALCL) where the tyrosine kinase domain is fused to nucleophosmin (NPM), a product of recurrent t(2;5)(p23;q35) chromosome translocation.⁶ Subsequently, chromosome rearrangements resulting in ALK fused to various partner genes have been found in nearly 70% of ALCL, 40-60% of inflammatory myofibroblastic tumors (IMT),⁷ a few dozen cases of diffuse large B-cell lymphoma (DLBCL), and most recently in 2-7% of non-small cell lung cancer (NSCLC).⁸⁻¹⁰ Among fusion partner genes identified to date, NPM is the most common partner in ALCL and echinoderm microtubule-associated protein-like-4 (EML4) is the main partner in NSCLC. In addition to the chromosome rearrangements that result in ALK fusion genes, amplification of ALK gene and activating point mutations in the full length ALK gene have recently been reported in neuroblastoma,¹¹⁻¹³ inflammatory breast cancer,¹⁴ and ovarian cancer.¹⁵

To date, **3** (crizotinib, Xalkori®)^{16, 17} has been approved for the treatment ALK-positive NSCLC and **2** (LDK378, ceritinib, Zykadia®)¹⁸ was approved for the treatment of crizotinib-resistant NSCLC patients. Both **4** (alectinib) and **5** (AP26113) have obtained the breakthrough therapy designation by the FDA for their activity in crizotinib-resistant NSCLC patients. Figure 1 represents a selected subset of ALKi currently FDA approved or in clinical trials.¹⁸⁻²⁵

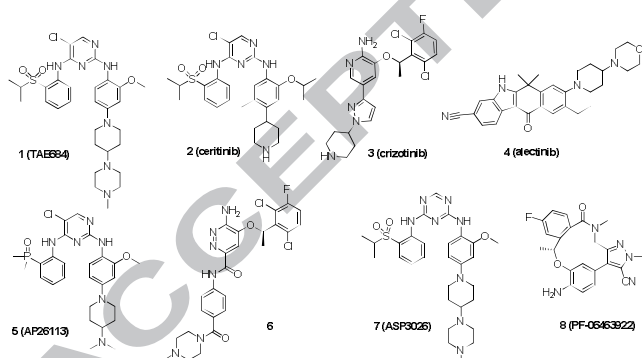


Figure 1. Selected examples of ALKi.

In a previous communication, we presented the modifications we made around TAE684 (**1**) that led to the discovery of LDK378 (**2**).¹⁸ We present additional medicinal chemistry efforts performed on this scaffold; focusing in this communication on the replacement of the pyrimidine ring present in compound **2** in the aim of optimizing hinge interactions.

2 binds to the hinge of the ALK kinase via interactions of the N1 of the pyrimidine ring and N2 from the aniline bearing the solubilizing moiety.²⁶ As we described previously, docking of **2** in the ALK kinase domain revealed the aminopyrimidine making contact at the hinge with the Met₁₁₉₉ residue and was

within reach of the carbonyl from the Glu₁₁₉₇ towards the gatekeeper region (Figure 2). This conformation was confirmed later on when a co-crystal was obtained.²⁶ We postulated it was likely feasible to introduce an extra interaction with Glu₁₁₉₇ by a simple addition of a hydrogen donor in this region. This would result into a hinge binding moieties containing three donor-acceptor interactions instead of two in the pyrimidine case.

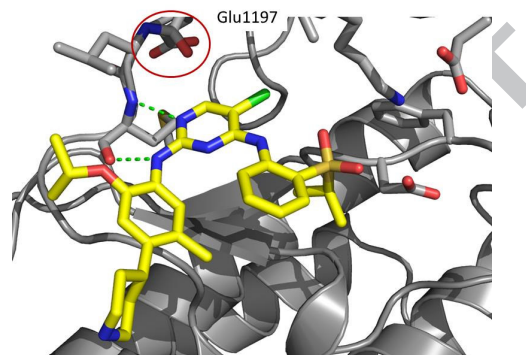


Figure 2. Co-crystal structure of **2** complexed with the ALK kinase domain depicting the proximity of Glu₁₁₉₇ to the pyrimidine ring forming interactions with Met₁₁₉₉ at the hinge moiety.²⁷

In the aim to conduct our studies (and further test our hypothesis), we decided to include some ring systems that lack the possibility to involve a third interaction at the hinge like a quinazoline (**F**) and a pyrimidopyrimidine (**G**) in addition to the 5,6-fused ring systems like a pyrrolopyrimidine (**A**), a purine (**B**), or a pyrazolopyrimidine (**D**). The ring systems and the anilines **II-III** we used to make the final molecules are depicted in Figure 3.

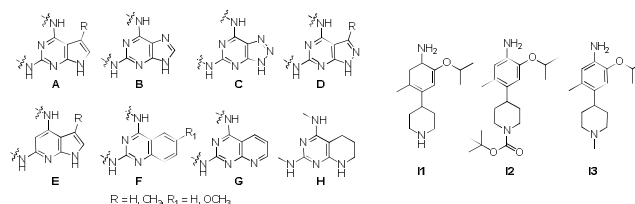
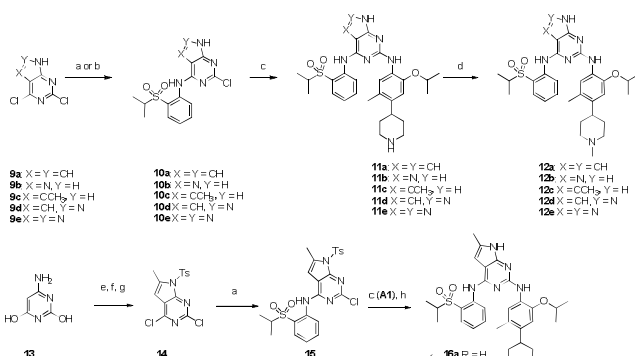


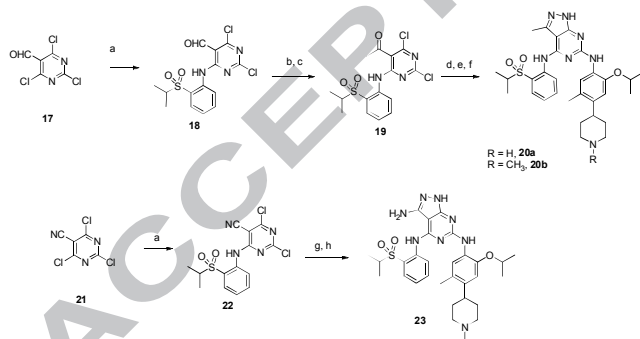
Figure 3. Rings systems (**A-H**) and anilines (**II-III**) used to make the final molecules.

The syntheses of the compounds described in this communication (**11a-e**, **12a-e**, **16a,b**, **20a,b**, **23**, **26**, **27**, **30a,b**, **31** and **32**) mirror the synthetic route we described for the synthesis of **2**¹⁸ and are depicted in schemes 1-4. For the sake of clarity, we have voluntarily restricted the analogues shown in this communication as ones bearing an unsubstituted piperidine (compounds **11a-e**, **16a**, **20a**, **31** and **33**) or *N*-Me-substituted piperidine ring (compounds **12a-e**, **16b**, **20b**, **23**, **26**, **27** and **30a,b**). Typically, we introduced the 2-(*iso*-propylsulfonyl)amino moiety first using simple amination conditions (usually, IPA, reflux) by condensation of **9a-e**, **14**, **17**, **21** and **28a-c** with 2-(*iso*-propylsulfonyl)aniline to afford **10a-e**, **15**, **18**, **22** and **29a-c** in moderate to excellent yields. In the case of compounds **11a-e**, **30a,b**, **29a-c** and **31** the synthesis was completed by a second amination reaction using selected proprietary aniline derivatives (**II-III**, Figure 3) in moderate to good yields.^{18,28} In the case of compounds **16a,b**, and **23**, an additional synthetic step was introduced on **18** and **22** in order to form the pyrazolopyrimidine ring (NH₂NH₂·2HCl, NaOAc, EtOH, 80°C). For compounds **16a**, **26** and **27**, an additional deprotection step of the tosylate and

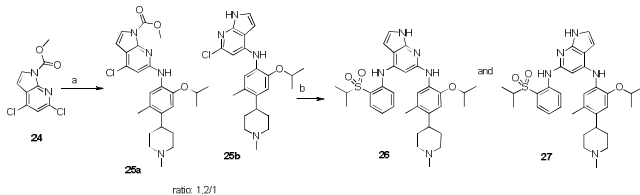
carbamate groups was necessary to complete the synthesis. Further alkylation (typically, $\text{CH}_3\text{-I}$, Et_3N , DMF, MW, 100°C , 10 minutes) of compounds **11a-e** afforded the derivatives **12a-e** in good yields (>70%). Reductive amination (HCHO, MeOH/THF, NaBH_3CN) of **16a** yielded compound **16b**. Compounds **26** and **27** required an inverted sequence of reactions in order to be synthesized (amination using 2-(*iso*-propylsulfonyl)aniline failed to produce the desired derivative, likely due to the lower reactivity of the aniline). Their synthesis was achieved by two sequential Buchwald couplings involving at first the aniline **13** and at second the 2-(*iso*-propylsulfonyl)amino moiety. Finally, reduction of the pyridine ring (PtO_2 , AcOH, TFA) of **31** yielded **32** in good yield.



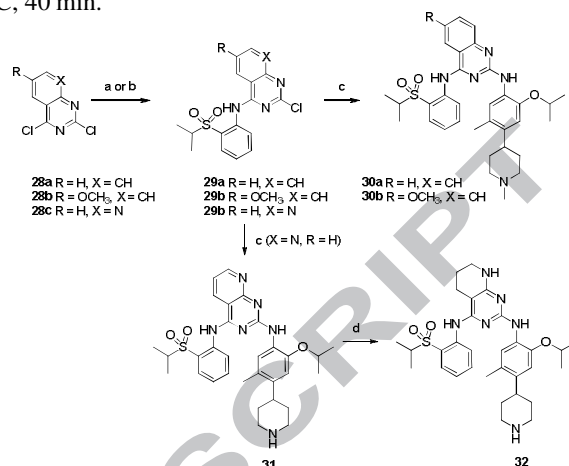
Scheme 1. Synthesis of derivatives **11a-e**, **12a-e**, and **16a,b**. Reagents and conditions: a. 2-(*iso*-propylsulfonyl)aniline, conc. HCl, IPA, 150°C MW. b. NaH, DMF/DMSO (10:1 v/v), 0°C to RT. c. **12**, conc. HCl, IPA, 160°C , MW, 30 min. d. $\text{CH}_3\text{-I}$, Et_3N , DMF, MW, 100°C 10 min. e. Chloroacetone (1.2 eq.), NaOAc (2.1 eq.), H_2O , reflux, 3 hr. f. POCl_3 , DIEPA, toluene, 70 to 110°C , O/N. g. (1) NaH, TsCl, DMF, 0°C , 1 hr. (2) 10% NH_4Cl . h. NaOMe/MeOH, 50°C , 2 hrs then RT O/N. i. HCHO (37%/H₂O), MeOH/THF (1/1 v/v), RT, 2 hrs followed by NaBH_3CN , RT, 30 min.



Scheme 2. Synthesis of derivatives **20a,b** and **23**. Reagents and conditions: a. 2-(*iso*-propylsulfonyl)aniline, conc. HCl, IPA, 150°C MW. b. CH_3MgBr , THF, -78°C to RT. c. PDC, DCM, RT. d. **12** or **13** conc. HCl, IPA, 160°C , MW, 30 min. e. $\text{NH}_2\text{NH}_2 \cdot 2\text{HCl}$, NaOAc, EtOH, 80°C . f. TFA/DCM. g. TFA, CH_2Cl_2 , RT. h. $\text{CH}_3\text{-I}$, Et_3N , DMF, MW, 100°C , 10 min. g. **13** conc. HCl, IPA, 160°C , MW, 30 min. h. NH_2NH_2 , IPA, reflux



Scheme 3. Synthesis of derivatives **26** and **27**. Reagents and conditions: a. Pd(OAc)₂, Xantphos, C_2CO_3 , THF, MW, 150°C , 40 min. b. **13**, Pd2(dba)₃, X-Phos, NaOtBu, THF, MW, 150°C , 40 min.



Scheme 4. Synthesis of derivatives **30a,b**, **31** and **32**. Reagents and conditions: a. 2-(*iso*-propylsulfonyl)aniline, conc. HCl, dioxane, 150°C MW. b. **13**, conc. HCl, $\text{CH}_3\text{CH}_2\text{CH}_2\text{OH}$, 160°C , MW, 20 min. d. H_2 , PtO_2 , AcOH, TFA.

As described in our previous communication,¹⁸ ALK inhibition was directly measured in a cellular context by measuring the proliferation of Ba/F3 cells expressing NPM-ALK as a guide for our SAR. Ba/F3 cells expressing the Tel-InsR fusion protein as well as wild-type (WT) Ba/F3 cells were used as counter screens. From our studies, several compounds (**11a**, **11d**, **12a-e** and **20a,b**) display IC_{50} s below 50 nM (47, 33, 6, 15, 8, 13, 47, 38 and 20 nM respectively) while eight compounds (**16a,b**, **26**, **27**, **30a,b**, **31** and **32**) suffer a strong loss in potency (684, 1298, 1427, 1119, 1082, 1286, 3172 and 1326 nM respectively). The other compounds (**11b**, **11c** and **23**) were moderately potent against ALK (114, 66 and 150 nM respectively). We were pleased to see that **12a-d** and **20b** were potent ALK inhibitors with IC_{50} s equal or below 20 nM (6, 15, 8, 13 and 20 nM respectively). From this study, it appeared quickly that most 6,5-fused ring systems tried were tolerated except when a substitution was introduced at the 2-position of the pyrrolopyrimidine core (compounds **16a,b**) or when one of the nitrogen from the bicyclic system was removed (compound **26** and **27**).³⁰ Typically, 6,6-fused ring system were not well tolerated (**30a,b**, **31** and **32**).³⁰ The result obtained with compound **31** was predictable due to the fact **31** contains an H-bond acceptor instead of an H-bond donor needed to form a hydrogen bond with the carbonyl of Glu₁₁₉₇. The low potency with compound **32** is likely due to a larger flexibility of the tetrahydropyridine moiety inducing a sub-optimal positioning of the NH bond towards Glu₁₁₉₇. All compounds show a moderate to good selectivity (20-76 fold) versus InsR (**12a** having the highest selectivity ratio of 76 fold) except for compounds **16a,b**, **26**, **27**, **30a,b**, **31** and **32** where the selectivity was mostly abrogated likely due to the sharp drop in potency for ALK. Typically, no significant viability impairment of BaF3 cells was observed (BaF3-WT column, table 1).

Compound	BaF3-NMP-ALK	BaF3-Tel-InsR	BaF3-WT
2	151 ± 18	1643 ± 272	3479 ± 180
1	26 ± 1	319 ± 24	2477 ± 448
11a	47 ± 3	700 ± 100	2216 ± 100
11b	114 ± 27	2700 ± 200	>10
11c	66 ± 9	938 ± 38	3521 ± 450
11d	33 ± 20	1913 ± 519	6220 ± 1230
12a	6 ± 1	455 ± 37	3422 ± 251
12b	15 ± 4	477 ± 60	3180 ± 1870
12c	8 ± 1	408 ± 39	4549 ± 680
12d	13 ± 1	703 ± 207	5120 ± 520
12e	47 ± 14	5058 ± 780	>10000
16a	684 ± 69	4390 ± 410	5411 ± 630
16b	1298 ± 152	3933 ± 560	5731 ± 760
20a	38 ± 4	1149 ± 200	5540 ± 600
20b	20 ± 7	429 ± 41	2507 ± 747
23	150 ± 13	3451 ± 970	4503 ± 900
26	1427 ± 151	5682 ± 700	4912 ± 550
27	1119 ± 150	1666 ± 281	2599 ± 532
30a	1082 ± 132	2232 ± 291	3240 ± 170
30b	1286 ± 91	2240 ± 460	3940 ± 110
31	3172 ± 350	5925 ± 720	7230 ± 700
32	1326 ± 80	2656 ± 1215	2033 ± 342

Table 1. Activity profile of compounds **11a-d**, **12a-e**, **16a,b**, **20a,b**, **23**, **26**, **27**, **30a,b**, **31** and **32**. All data given in nM and are an average of duplicate measurements.

Since we did observe a poorer activity in Ba/F3 cells for some of the derivatives described in Table 1, we ran a subset of these compounds in the Karpas299 cell line (patient cell line harboring the NMP-ALK fusion) as well as an enzymatic ALK assay in order to confirm their poor cellular potency was due to a lower affinity for ALK and not due to other parameters such as cell permeability. The results of this selected set of compounds tested are described in Table 2. These two assays show a strong correlation with each other and also with the BaF3 results (moderately to highly potent derivatives have similar IC₅₀s on all assays (**11b**, **11c**, **12a,b** and **20a,b**) while weak derivatives from our Ba/F3 SAR driving assay show a much weaker activity in both Karpas299 and ALK enzyme assay (**16a**, **26**, **27**, **30b** and **32**).

Compound	Karpas299	ALK enzyme
2	64 ± 6	7 ± 1
11b	118 ± 13	2 ± 0.3
11c	57 ± 18	20 ± 0.3
12a	3 ± 0.8	8 ± 0.2
12b	6 ± 1	2 ± 0.2
16a	328 ± 30	3878 ± 1110
20a	7 ± 0.2	5 ± 1.0
20b	26 ± 4.4	4 ± 0.1
26	7310 ± 1180	>25000

27	2867 ± 862	186 ± 10
30b	1344 ± 405	1930 ± 320
32	6851 ± 2311	212 ± 13

Table 2. Activity of selected derivatives against the Karpas299 cancer cell line and ALK enzyme.

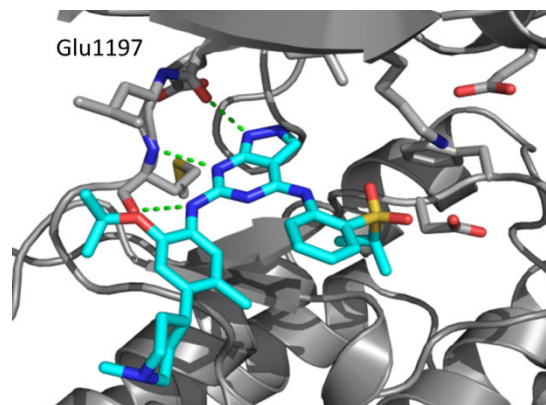


Figure 4. Co-crystal structure of **12d** complexed to the ALK kinase domain.²⁹ A clear H-bond is visible between GLU₁₁₉₇ and the hydrogen from the pyrazolopyrimidine ring.

The co-crystal structure of **12d** with ALK was obtained and shown in Figure 4. There is a clear hydrogen bond between the NH of the pyrazolopyrimidine ring and the carbonyl of GLU₁₁₉₇. This experimental structure confirmed our hypothesis and also correlated well with the SAR observed with the compounds described.

A selected set of these derivatives were tested for their ADME profile (metabolic clearance, CYP3A4 inhibition, HT-solubility at pH 6.8, PAMPA, Caco2 and hERG binding). The results are summarized in Table 3. All compounds displayed a low to moderate microsomal clearance. CYP inhibition was typically moderate (around 5 μM for most derivatives) and ranged from about 3 μM (**12d**) to >25 μM (**20b**). A wide range of solubility profiles were also observed (from 8 to >175 μM) which did not correlate well with the basicity of the amine present on the piperidine ring. For example, **12a** and **12b** have the same N-methyl piperidine moiety (identical calculated pK_as of 9.48) but have a drastic different solubility profile (10.4 versus >175 μM). Most compounds had good permeability (PAMPA) except **11a**. **11a** and **12b-c** showed an efflux potential in the caco2 assay. hERG binding IC₅₀s were also quite widespread, ranging from 1 μM (**11a** and **12d**) to >30 μM (**20b**). Overall, compound **20b** appeared to have a superior profile compared to the other compounds listed in Table 3 and proved to be very selective for ALK. When tested enzymatically against a panel of 28 kinases (Table 3), **20b** displayed IC₅₀ below 1 μM for only the following 3 kinases: IGF-1R, CDK2 and HER1 (0.47, 0.92 and 0.96 μM respectively).

Kinase	IC ₅₀	Kinase	IC ₅₀
NPM-ALK	0.03	EphB4	2.9
EML4-ALK	0.01	FGFR4	>10
BTK	9.4	FGFR3	>10

ABL	1.4	HER1	0.96
AKT	7.6	HER2	7.8
Aurora	>10	IGF-1R	0.47
CDK2	0.92	KDR	7.4
GSK3 β	4.3	LCK	4.3
JAK1	>10	PDGFR α	9.7
JAK2	>10	PDK1	>10
JAK3	>10	RET	3.6
MAPK1	>10	SYK	>10
PLK1	3.9	cKit	>10
TYK2	>10	MET	8.1
EphA4	>10		

Table 3. Enzymatic profile of compound **20b**. All data given in nM and are an average of duplicate measurements.

Table 5 shows the *in vivo* mouse and rat PK profile of compounds **11a**, **12a-c** and **20b** (**11a** and **12b** were not tested for their rat PK due to their poor PK properties in mice). All compounds display a moderate clearance in mice (40-71 mL/min/kg), and rats (15-32 mL/min/kg), they tend to have a high V_{ss} (7-19 L/kg) except **12b** which had a much lower V_{ss} in mice (2.4 L/Kg). All compounds had a relatively low C_{max} in mice (29-429 nM) and rats (151-291 nM) and a moderate bioavailability in both species (35-58%) which typically was higher in mice, except for **9a** and **10b** which show a very poor bioavailability in mice.

Based on these data, we decided to evaluate **20b** in a two week Karpas299 SCID mice xenograft model harboring the NMP-ALK fusion (Figure 5). When dosed once a day at doses of 25 and 50 mg/kg, **20b** demonstrated a dose-dependent anti-tumor activity with significant tumor regression at 50 mg/kg.³¹ Tumor changes were measured as %T/C where changes in tumor weight for each treated (T) and control (C) groups were measured and a percent of the ratio was calculated. Tumor shrinkage (37% T/C) was observed at 25 mg/kg and tumor regression (-54% T/C) was observed at 50 mg/kg. All doses were well tolerated with no body weight loss (data not shown).

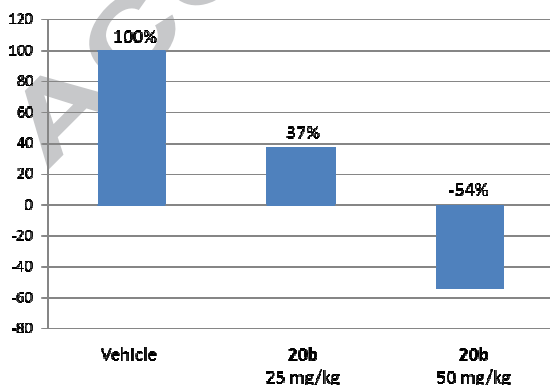


Figure 5. **20b** activity in SCID mice Karpas299 xenograft.²⁷

In conclusion, we successfully designed and synthesized novel potent ALKi based on structural information available from the 2,4-diaminopyrimidine hinge-binding moiety present in ceritinib. The design was directed towards the morphing of the pyrimidine ring contained in **2** into various bicyclic systems that possess an additional interaction at the hinge with Glu1197 allowed us to reach our goal in identifying potent derivatives such as **12a-d** or **20b**. Compound **20b** possesses an attractive profile (potent on target, high selectivity against other kinases, good solubility, low hERG inhibition, low CYP inhibition), has an acceptable pharmacokinetic profile in mice and rats and induces tumor regression in a Karpas299 xenograft mouse model of ALCL at 50 mg/kg when dosed once a day.

compound	CL _{int} , m, r, h ¹	CYP3A4 ²	HT-sol. ³	Log PAMPA ⁴	Caco2 (A-B/B-A)	hERG ⁵
11a	15, 14, 22	4.6 ± 0.9	8.1	-5.7 (ND)	0.04/1.3*	1.1
12a	62, 34, 25	4.5	10.4	<-3.3 (99.8)	1.3/1.1	1.7
12b	52, 28, 45	5.7	>175	-5 (92.3)	1.1/9.4*	19.0
12c	7, ND, 29	5.1	30.9	-4.9 (75)	0.6/0.3**	8.6
12d	37, 30, 32	3.3	>175	-4.1	2.6/3.1	1.0
20b	13, 33, 19	>25	114	-4.9 (99.6)	2.1/3.3	20.8

Table 4. ADME profile of selected derivatives.¹ Intrinsic Clearance (CL_{int}) is in $\mu\text{L}/\text{min}/\text{mg}$ in liver microsomes.² IC₅₀ data in μM . Inhibition measured using midazolam as substrate.³ Data in μM measured from DMSO solution in buffer adjusted to pH6.8.⁴ Permeability is in cm/sec. ⁵ IC₅₀ data in μM in dofetilide binding assay. * Efflux. ** Poor recovery (<30%).

Parameter	Mouse PK					Rat PK				
	CL ¹	V _{ss} ²	C _{max} ³ (PO)	AUC ⁴ (PO)	%F	CL	V _{ss}	C _{max}	AUC	%F
11a	40	7.3	51	406	3	ND	ND	ND	ND	ND
12a	58	10.8	425	5980	59	15	13.7	291	7187	35
12b	59	2.4	29	123	2	ND	ND	ND	ND	ND
12c	55	11.0	300	4959	47	19	17.3	189	3268	24
20b	71	12.1	429	4899	58	32	19.4	151	3071	35

Table 5. Mouse and rat PK profile of compounds **11a**, **12a-c** and **20b**. ¹ mL/min/kg. ² L/kg. ³ nM. ⁴ hrs*nM

Acknowledgments

The authors would like to thank Paul Calvin the compound management group, John Isbell and the ADME and analytical groups, Todd Groessel and the DMPK bioanalytical group, Muyun Gao and Ken Ng and the Protein Sciences group, Frank Sun and the Oncology Pharmacology group.

References and notes

- Morris, S. W.; Naeve, C.; Mathew, P.; James, P. L.; Kirstein, M. N.; Cui, X.; Witte, D. P. ALK, the chromosome 2 gene locus altered by the t(2;5) in non-Hodgkin's lymphoma, encodes a novel neural receptor tyrosine kinase that is highly related to leukocyte tyrosine kinase (LTK). *Oncogene*. **1997**, *14*, 2175.
- Chiarle, R.; Voena, C.; Ambrogio, C.; Piva, R.; Inghirami, G. *Nature Rev. Cancer*. **2008**, *8*(1), 11.
- Webb, T. R.; Slavish, J.; George, R. E.; Look, A. T.; Xue, L.; Jiang, Q.; Cui, X.; Rentrop, W. B.; Morris, S. W. *Expert Rev. Anticancer Ther.* **2009**, *9*(3), 331-.
- Iwahara T.; Fujimoto J.; Wen D.; Cupples R.; Bucay N.; Arakawa T.; Mori S.; Ratzkin B.; Yamamoto T. *Oncogene*. **1997**, *14*, 439.
- Bilsland J. G.; Wheeldon A.; Mead A.; Znamenskiy P.; Almond S.; Waters K. A.; Thakur M.; Beaumont V.; Bonnert T. P.; Heavens R.; Whiting P.; McAllister G.; Munoz-Sanjuan I. *Neuropsychopharmacology*. **2008**, *33*, 685.
- Morris S. W.; Kirstein M. N.; Valentine M. B.; Dittmer K. G.; Shapiro D. N.; Saltman D. L.; Look A. T. *Science*. **1994**, *263*, 1281.
- Griffin, C. A.; Hawkins, A. L.; Dvorak, C.; Henkle, C.; Ellingham, T.; Perlman, E. J. *Cancer Res*. **1999**, *59*, 2776.
- Soda, M.; Choi, Y. L.; Enomoto, M.; Takada, S.; Yamashita, Y.; Ishikawa, S.; Fujiwara, S.; Watanabe, H.; Kurashina, K.; Hatanaka, H.; Bando, M.; Ohno, S.; Ishikawa, Y.; Aburatani, H.; Niki, T.; Sohara, Y.; Sugiyama, Y.; Mano, H. *Nature*. **2007**, *448*, 561.
- Mano, H. *Cancer Sci*. **2008**, *99*, 2349.
- Shaw, A. T.; Solomon, B. *Clin. Cancer Res*. **2011**, *17*(8), 2081.
- Osajima-Hakomori, Y.; Miyake, I.; Ohira, M.; Nakagawara, A.; Nakagawa, A.; Sakai, R. *Am. J. Pathol.* **2005**, *167*, 213.
- Mosse, Y. P.; Laudenslager, M.; Longo, L.; Cole, K.A.; Wood, A.; Attiyeh, E. F.; Laquaglia, M. J.; Sennett, R.; Lynch, J. E.; Perri, P.; Laureys, G.; Speleman, F.; Kim, C.; Hou, C.; Hakonarson, H.; Torkamani, A.; Schork, N. J.; Brodeur, G. M.; Tonini, G. P.; Rappaport, E.; Devoto, M.; Maris, J. M. *Nature*. **2008**, *455*, 930.
- Azarova, A. M.; Gautam, G.; George, R. E. *Seminars in Cancer Bio*. **2011**, *21*, 267.
- Tuma, R. S. *J. Nat. Cancer Inst.* **2012**, *104*(2), 87-88.
- Ren, H.; Tan, X. Z.; Crosby, C.; Haack, H.; Ren, J.-M.; Beausoleil, S.; Moritz, A.; Innocenti, G.; Rush, J.; Zhang, Y.; Zhou, X.-M.; Gu, T.-L.; Ynag, Y.-F.; Comb, M. J. *Cancer Res*. **2012**, *72*, 3312.
- Christensen, J. G.; Zou, H. Y.; Arango, M. E.; Li, Q.; Lee, J. H.; McDonnell, S. R.; Yamazaki, S.; Alton, G. R.; Mroczkowski, B.; Los, G. *Mol. Cancer Therapeutics*. **2007**, *6*(12), 3314.
- Cui, J. J.; Tran-Dube, M.; Shen, H.; Nambu, M.; Kung, P.-P.; Pairish, M.; Jia, L.; Meng, J.; Funk, L.; Botrous, I.; McTigue, M.; Grodsky, N.; Ryan, K.; Padriue, E.; Alton, G.; Timofeevski, S.; Yamazaki, S.; Li, Q.; Zou, H.; Christensen, J.; Mroczkowski, B.; Bender, S.; Kania, R. S.; Edwards, M. P. *J. Med. Chem.* **2011**, *54*(18), 6342.
- Marsilje, T. H.; Pei, W.; Chen, B.; Lu, W.; Uno, T.; Jin, Y.; Jiang, T.; Kim, S.; Li, N.; Warmuth, M.; Sarkisova, Y.; Sun, F.; Steffy, A.; Pferdekamper, A. C.; Li, A. G.; Joseph, S. B.; Kim, Y.; Liu, T.; Tuntland, T.; Cui, X.; Gray, N. S.; Steensma, R.; Wan, Y.; Jiang, J.; Chopiuk, G.; Li, J.; Gordon, W. P.; Richmond, W.; Johnson, K.; Chang, J.; Groessel, T.; He, Y.-Q.; Phimister, A.; Aycinena, A.; Lee, C. C.; Bursulaya, B.; Karanewsky, D. S.; Seidel, H. M.; Harris, J. L. and Michellys, P.-Y.; *J. Med. Chem.*, **2013**, *56* (14), pp 5675.
- Sakamoto, H.; Tsukaguchi, T.; Hiroshima, S.; Kodama, T.; Kobayashi, T.; Fukami, T. A.; Oikawa, N.; Tsukuda, T.; Ishii, N.; Aoki, Y. *Cancer Cell*. **2011**, *19*, 679.
- Kinoshita, K.; Kobayashi, T.; Asoh, K.; Furuichi, N.; Ito, T.; Kawada, H.; Hara, S.; Ohwada, J.; Hattori, K.; Miyagi, T.; Hong, W.-S.; Park, M.-J.; Takanashi, K.; Tsukaguchi, T.; Sakamoto, H.; Tsukuda, T.; Oikawa, N. *J. Med. Chem.* **2011**, *54*, 6286.
- Kuromitsu, S.; Mori, M.; Shimada, I.; Kondoh Y.; Shindoh N.; Soga T.; Furutani T.; Konagai S.; Sakagami H.; Nakata M.; Ueno Y.; Saito R.; Sasamata M.; Kudou M. American Association for Cancer Research (AACR) Annual Meeting in Orlando, Florida. 2011, abstract #2821.
- Lovly, C. M.; Heuckmann, J. M.; De Stanchina, E.; Chen, H.; Thomas, R. K.; Liang, C.; Pao W. *Cancer Res*. **2011**, *71*(14), 4920.
- Katayama, R.; Khan, T. M.; Benes, C.; Lifshits, E.; Eb, H.; River, V. M.; Shakespeare, W. C.; Iafate, A. J.; Jeffrey A. Engelman; J. A., Shaw, A. T. *Proceed. Nat. Acad. Sci. USA*. **2011**, *108*(18), 7535.
- Rivera, V. M.; Anjum, R.; Wang, F.; Zhang, S.; Keats, J.; Ning, Y.; Wardwell, S. D.; Moran, L.; Ye, E.; Chun, D. Y.; Mohemmad, K. Q.; Liu, S.; Huang, W.-S.; Wang, Y.; Thomas, M.; Li, F.; Qi, J.; Miret, J.; Iulicucci, J. D.; Dalgarno, D.; Narasimhan, N. I.; Clackson, T.; Shakespeare, W. C. American Association for Cancer Research (AACR) Annual Meeting in Washington, D.C., 2010, abstract #3623.
- Johnson, T. W.; Richardson, P. F.; Bailey, S.; Brooun, A.; Burke, B. J.; Collins, M. R.; Cui, J. J.; Deal, J. G.; Deng, Y.-L.; Dinh, D.; Engstrom, L. D.; He, M.; Hoffman, J.; Hoffman, R. L.; Huang, Q.; Kania, R. S.; Kath, J. C.; Lam, H.; Lam, J. L.; Le, P. T.; Lingardo, L.; Liu, W.; McTigue, M.; Palmer, C. L.; Sach, N. W.; Smeal, T.; Smith, G. L.; Stewart, A. E.; Timofeevski, S.; Zhu, H.; Zhu, J.; Zou, H. Y.; Edwards, M. P.; *J. Med. Chem.*, **2014**, *57* (11), 4720.
- Friboulet, L., Li, N., Katayama, R., Lee, C., Gainor, J. F., Crystal, A. S., Michellys, P.-Y., Awad, M. M., Yanagitani, N., Kim, S., Pferdekamper A. C., Li, J., Kasibhatla, S., Sun, F., Sun, X., Hua, S., McNamara, P., Mahmood, S., Lockerman, E. L., Fujita, N., Nishio, M., Harris, J. L., Shaw, A. T., Engelman, J. A., *Can. Disc.* **2014**, *10*, 662.

27. PDB code 4MKC.

28. Chen, B.; Jiang, T.; Marsilje, T. H.; Michellys, P.-Y.; Nguyen, T. N.; Pei, W.; Wu, B.; Gao, Z.; Ge, Y.; Huang, C.; Li, Y.; WO 2009126515 A1

29. PDB code 4Z55.

30. No attempts were done to try to improve activity using these single bicyclic hinge moieties; since both 24 and 25 possess a hinge binding moiety, it may be possible to re-optimize the compounds using divergent SAR directions.

31. The study was intended to be conducted for 2 weeks. However, due to the very aggressive growth rate of these tumors, the vehicle animals were sacrificed after 9 days for humane reasons.

ACCEPTED MANUSCRIPT